Journal of Food Engineering 413 (2026) 112989

Contents lists available at ScienceDirect

Journal of Food Engineering

journal homepage: www.elsevier.com/locate/jfoodeng

Moisture adsorption characteristics of freeze-dried royal jelly: thermodynamic properties, modeling, and assessing microstructural changes

Rachida Ouaabou [a], Lahcen Hssaini [b], Abderrahim Alahyane [c,d], Abdessamad Lahrach [e], Nadia Massaoudi [f], Jalal Isaad [a], EL amine Ajal [g], Aadil Bajoub [f], Said Ennahli [f,*]

[a] ERCI2A, FSTH, Abdelmalek Essaadi University, Tetouan, 93000, Morocco
[b] Agro-Food Technology and Quality Laboratory, Regional Center of Agricultural Research of Meknes, National Institute of Agricultural Research, Rabat, 10090, Morocco
[c] Higher Institute of Nursing Professions and Health Techniques of Guelmim, Morocco
[d] Laboratory of Water Sciences, Microbial Biotechnologies, and Natural Resource Sustainability, Faculty of Sciences Semlalia, Cadi Ayyad University, Marrakesh 40000, Morocco
[e] Faculty of Sciences Semlalia, Cadi Ayyad University, Marrakech, 40000, Morocco
[f] Ecole Nationale d'Agriculture de Meknès (ENAM), Meknes, 50001, Morocco
[g] Mohammed V University, Faculty of Medicine and Pharmacy, Rabat, Morocco

ARTICLE INFO

Keywords:
Sorption isotherms
Royal jelly
Equilibrium moisture content
Integral thermodynamic properties
Storage stability

ABSTRACT

This study aimed to investigate the sorption characteristics of royal jelly (RJ) to better understand how it interacts with moisture under varying conditions. We employed gravimetric static techniques to generate sorption isotherms, using chemical salts to precisely control water activity (a_w) over a range of 0.05–0.90. The experiments were conducted at three different temperatures 30 °C, 40 °C, and 50 °C. To gain further insights, we applied the Clausius-Clapeyron equation to calculate the integral thermodynamic properties of the RJ water system under constant spreading pressure. Our goal was to determine the best storage conditions to maintain the quality and extend the shelf life of royal jelly powder.

The results showed that royal jelly's sorption isotherms followed a Type II sigmoidal pattern, meaning that moisture content increased as water activity rose. Among the models we tested, the Enderby model provided the most accurate fit to our experimental data. Furthermore, the analysis of integral entropy revealed a minimum value when the moisture content ranged between 4 and 5 % (dry basis) and the relative humidity was between 0.15 and 0.23. These specific conditions were identified as ideal for prolonging the shelf life and preserving the quality of royal jelly. Scanning Electron Microscopy revealed an agglomerated structure, and thermal analysis showed a multi-stage degradation process, with the major mass loss occurring above 246 °C. Overall, this comprehensive investigation into RJ's sorption properties, including a detailed assessment of its thermodynamic behavior, offers valuable insights for optimizing its storage and preservation, ensuring the integrity of this highly nutritious food product.

1. Introduction

Royal jelly (RJ) is a nutrient-dense secretion produced by nurse bees (*Apis mellifera*), primarily used to nourish both developing larvae and the queen bee. Rich in proteins, lipids, vitamins, and various bioactive compounds, RJ has garnered significant attention in the pharmaceutical and cosmetic industries for its potential health benefits, including antioxidant, anti-inflammatory, and antimicrobial effects (Ramadan and Al-Ghamdi, 2012; Melliou, 2014; Fratini et al., 2016; Chen et al., 2023).

As a commercial product, royal jelly is commonly available in liquid form (refrigerated or frozen), as capsules, or in powder form (lyophilized, i.e. freeze-dried). The powder form is particularly advantageous for long-term storage, dosage standardisation, and incorporation into other products, including tablets, functional foods, and nutraceuticals.

* Corresponding author.
E-mail address: ennahlisaid@gmail.com (S. Ennahli).

https://doi.org/10.1016/j.jfoodeng.2026.112989
Received 24 August 2025; Received in revised form 10 December 2025; Accepted 13 January 2026
Available online 20 January 2026

From a regulatory perspective, royal jelly is categorised as a dietary supplement in numerous countries, including the United States, where it is widely accepted as safe (GRAS) for its designated use. Within the European Union, the substance is regulated as a foodstuff and is subject to novel food regulations in certain contexts. Conversely, in other regions, such as Japan and Australia, it has been approved for use in health supplements and listed medicines (Ramadan and Al-Ghamdi, 2012; Khazaei et al., 2018).

A key challenge in fully utilizing RJ's benefits lies in understanding its hygroscopic nature how it interacts with moisture. This understanding is crucial for optimizing preservation techniques like freeze-drying, which is essential for extending RJ's shelf life and maintaining its quality attributes during storage. This includes preserving the stability of bioactive compounds (e.g. 10-HDA and major royal jelly proteins), sensory properties (e.g. flavour, colour, aroma) and physical structure, since all of these are highly susceptible to degradation from moisture uptake (Ramanathan et al., 2018).

In food science, sorption isotherms play a critical role, describing the relationship between water content and water activity at a given temperature. These isotherms help predict how RJ behaves under different humidity conditions (Ouaabou et al., 2021, 2022; Tagnamas et al., 2024). Analyzing these patterns also provides insight into RJ's thermodynamic properties, such as the isosteric heat of sorption, differential entropy, and spreading pressure factors vital for determining RJ's stability and performance across various environments (Aviara and Igbeka, 2016; Hssaini et al., 2022).

Freeze-drying, or lyophilization, is a widely applied method for preserving RJ. The process involves freezing RJ and then reducing the surrounding pressure, causing the frozen water to sublimate directly into a gas, by passing the liquid phase. This method preserves RJ's structural integrity and bioactivity while minimizing microbial growth and enzymatic degradation risks (Ratti, 2001). To assess the effectiveness of freeze-drying, it is important to examine the microstructural changes RJ undergoes during the process and its subsequent storage.

Several models, including the Guggenheim-Anderson-de Boer (GAB), Halsey, and Smith models, have been proposed to describe the sorption behavior of food products. These models are crucial for predicting moisture content at different water activities, which in turn helps in designing appropriate packaging and storage solutions (Ouaabou et al., 2022; Tagnamas et al., 2024).

The microstructure of freeze-dried RJ also affects its hygroscopic behavior. Techniques like scanning electron microscopy (SEM), and thermal gravimetric-differential thermal analysis (TGA-DTA) allow for visualizing these structural changes, enabling us to link them to moisture absorption patterns.

Previous studies have emphasized the importance of water sorption properties in maintaining RJ's stability and shelf life (Moraga et al., 2012; Ornelas-Paz and Yahia, 2014; Jung et al., 2018). highlighted that controlling moisture content is essential for preserving the bioactive compounds and overall quality of freeze-dried products. This insight is vital for developing packaging and storage systems that prolong RJ's potency and efficacy. However, while the importance of moisture control is recognized, a critical gap exists in the fundamental understanding of royal jelly's water interactions. The extensive bioactivities of RJ are well-documented, but a systematic study linking its fundamental hygroscopic and thermodynamic properties to practical storage stability is lacking.

This study provides the first comprehensive thermodynamic and microstructural analysis of freeze-dried RJ, we investigate the hygroscopic properties of freeze-dried royal jelly by analyzing its sorption isotherms at various temperatures. By fitting the data to different models, we seek to identify the most accurate predictor of RJ's moisture sorption behavior. Additionally, we will examine its thermodynamic properties and microstructural changes to better understand how to preserve the quality and stability of this valuable substance.

2. Materials and methods

2.1. Material

Royal jelly (RJ) samples were obtained from a local beekeeper in the Meknes region of Morocco. A quantity of 250 g of the fresh royal jelly was placed in a laboratory freezer adjusted at −20 °C for 24h and transferred to a freeze-dryer (Alpha1-4LD plus). The lyophilization protocol consisted of a primary drying phase at 4.5Pa and −55 °C to sublime the frozen free water, followed by a secondary drying phase where the temperature was raised to 30 °C under reduced pressure to desorb the remaining bound water. The total lyophilization time was 96h.

2.2. Sample preparation

Following lyophilization, the royal jelly powder was homogenized with an electric grinder and stored in a sealed glass vial under ambient conditions (25 ± 2 °C and 40 ± 5 % RH). The powder was characterized immediately after preparation by adsorption isotherm analysis, SEM, and TGA-DTA to minimize the impact of storage on its initial microstructure and thermal properties.

2.3. Characterization techniques

The microstructure of RJ was analyzed using a scanning electron microscope (SEM), specifically a TESCAN VEGA 3 operating at 20 kV. Prior to imaging, the freeze-dried samples were gently ground into small fragments to fit the SEM sample holder and to obtain a representative surface for observation. The samples underwent carbon sputtering before being digitized and photographed at various magnifications (× 2.0K, × 600K, × 950K). To examine the thermal characteristics of the royal jelly, thermal gravimetric-differential thermal analysis (TG-DTA) was utilized employing a DTA, Labsys Evo 1600, SETARAM instrument. The procedure involved heating approximately 50 mg of the sample, contained in a platinum crucible, from room temperature (~25 °C) up to 800 °C at a constant heating rate of 10 °C min^{-1}. Both the SEM and thermal analyses were conducted exclusively on the initial freeze-dried powder.

2.4. Sorption isotherms protocol

Adsorption isotherms were determined using the static gravimetric method with saturated salt solutions. A total of eighteen 1L sealed desiccators were used (six different salts × three temperatures), each containing 200 mL of a different saturated salt solution to maintain a specific relative humidity (RH). The water activity (a_w) of these solutions ranged from 0.074 to 0.898, 0.063 to 0.891, and 0.057 to 0.882 at 30 °C, 40 °C, and 50 °C, respectively. Table 1 details the relative equilibrium moisture values of each salt solution as a function of temperature.

The temperatures selected for this study were determined to encompass the range of conditions that royal jelly might realistically encounter during storage, handling and transportation. These temperatures ranged from controlled room temperature (30 °C) to higher temperatures often experienced in warmer climates or during transit (40–50 °C).

Table 1
Selected saturated salt solutions and corresponding relative humidities (%) as a function of temperature (Bizot and Multon, 1978).

	KOH	$MgCl_2,6H_2O$	K_2CO_3	$NaNO_3$	KCl	$BaCl_2,2H_2O$
30 °C	7.38	32.38	43.17	72.75	83.62	89.80
40 °C	6.26	31.59	42.30	71.00	82.32	89.10
50 °C	5.72	30.54	40.91	69.04	81.20	88.23

A 0.5g sample of royal jelly was placed in a small, open container, which was then positioned inside one of the desiccators. To prevent fungal growth on the samples for salt solutions with high water activity (a_w>0.6), 2 mL of toluene was added to the desiccators. The desiccators were placed in an oven maintained at a specified temperature (±1 °C). The mass of the royal jelly samples was measured every two days. Equilibrium was considered achieved when a constant mass was reached, as indicated by three consecutive identical measurements. At this point, the samples were weighed to obtain the wet mass (Mh) and then transferred to a drying oven at 105 °C for 7h to determine the dry mass (Ms).

Finally, the equilibrium moisture content (EMC) of the product at hygroscopic equilibrium was determined using a specific equation:

$$\mathrm{EMC} = X_{eq} = \frac{M_h - M_s}{M_s} \times 100 \quad (1)$$

Where, M_h is the equilibrium mass at constant water activity and temperature (g). M_s is the dry mass after dehumidification at 105 °C (g). EMC is the equilibrium moisture content (% dry matter (db)).

2.5. Modeling equations

Five mathematical models were employed to analyze the moisture sorption isotherms of RJ. Specifically, the Guggenheim-Anderson-Boer (GAB), Halsey, Smith, Enderby, and Caurie equations were considered (Table 2).

2.6. Statistical analysis

The data were analyzed in triplicate (n = 3) and demonstrated as means ± SD (standard deviation). Model fitting and parameter estimation were performed using Curve Expert Professional (version 2.3). The goodness of fit for each model was evaluated using the correlation coefficient (r) and the mean relative error (MRE), as defined in equations (2) and (3).

$$r = \sqrt{\frac{\sum_{i=1}^{N}\left(X_{eq_{i,pred}} - \overline{X}_{eq_{i,exp}}\right)^2}{\sum_{i=1}^{N}\left(X_{eq_{i,exp}} - \overline{X}_{eq_{i,exp}}\right)^2}} \quad (2)$$

$$MRE = \frac{100}{N} = \sum_{i=1}^{N}\left|\frac{X_{eq_{i,exp}} - X_{eq_{i,pred}}}{X_{eq_{i,exp}}}\right| \quad (3)$$

Where,

$X_{eqi,exp}$ represents the measured experimental moisture content, expressed as a percentage on a dry basis (% db), $X_{eqi,\ pred}$ denotes the corresponding predicted moisture content, also in % db and N represent the number of data points.

Table 2
Mathematical models for analyzing moisture sorption isotherms of royal jelly.

Models	Mathematical expression	References
GAB	$Xeq = \frac{X_0 kCa_w}{(1-ka_w).(1-ka_w+kCa_w)}$	Van Den Berg and Bruin (1981)
Halsey	$Xeq = \left(\frac{-A}{ln\ a_w}\right)^{\frac{1}{B}}$	Halsey (1948)
Smith	$Xeq = A - B.(\ln(1-a_w))$	Smith and Smith (1947)
Enderby	$Xeq = \left[\frac{A}{1-Ba_w} + \frac{C}{1-Da_w}\right]a_w$	Popovski and Mitrevski (2004)
Caurie	$Xeq = exp(A + Ba_w)$	Castillo et al. (2003)

2.7. Calculation of integral properties for RJ

2.7.1. Spreading pressure

The thermodynamic properties are assessed under a constant spreading pressure, which is the force exerted in the plane of the surface to prevent diffusion. This pressure is indicative of the surface excess energy and is understood as the increase in surface tension at bare sorption sites due to the adsorption of molecules (Pascual Pineda et al., 2021a; Francisco-Ponce et al., 2025). This critical parameter is determined through an analytical process that takes into account both the moisture content and water activity.

$$\pi = \frac{K_B T}{A_m}\int_0^{a_w}\frac{\theta}{a_w}da_w \quad (4)$$

Where: k_B is Boltzmann constant (1.380×10^{-23} JK^{-1}), A_m is the surface area of a water molecule (1.06×10^{-19} m^2), the moisture ratio θ is given by $\theta = X_{eq}/X_0$, T (K) temperature. X_{eq} is the equilibrium moisture content and X_0 (kg (kg d.b.)$^{-1}$) is the monolayer moisture content.

By employing the GAB model's formula and replacing θ/a_w, it is possible to determine the integral spreading pressure. The substitution and integration process described in equation (4) can be analytically resolved, resulting in the mathematical definition for π as shown in equation (5):

$$\pi = \frac{K_B T}{A_m} ln\left[\frac{1 + Cka_w - ka_w}{1 - ka_w}\right] \quad (5)$$

Where k and C are the constants of GAB model.

2.7.2. Integral thermodynamic properties

The integral enthalpy (ΔH_i) denotes the additional energy needed during the sorption process beyond the heat of vaporization of water and is computed from experimental data using the Clausius–Clapeyron equation (Eq. (6)). This value offers significant information about the interaction strength between water and solids relative to the interactions among water molecules. Analogous to the differential enthalpy of sorption, the integral enthalpy is assessed at a constant spreading pressure. Under this condition, the integral enthalpy is derived from the Clausius-Clapeyron equation, as shown in Eq. (6) (Bahammou et al., 2020).

$$\left.\frac{\partial \ln(a_w)}{\partial\left(\frac{1}{T}\right)}\right|_{\varnothing} = \frac{\Delta H_i}{R} \quad (6)$$

The universal gas constant is represented by R (J/mol K), while ΔH_i signifies the integral enthalpy at a constant spreading pressure value (J/m^2). In practical terms, the integral enthalpy values were determined by plotting $\ln(a_w)$ against 1/T. For each spreading pressure value, the slope of this plot, given by ΔHi/R, yielded the integral enthalpy. To ascertain the integral entropy (ΔS_i), equation (7) was utilized. The integral entropy is a critical parameter for identifying the optimal biological stability zone for RJ. The calculation of the integral entropy was conducted using the following equation:

$$(\Delta S_i)_T = \frac{\Delta H_i}{T} - Rln(a_w) \quad (7)$$

Analyzing integral thermodynamic properties such as enthalpy and entropy enabled the determination of conditions where the minimum integral entropy value for RJ was achieved. A lower (minimum) ΔSi value indicates stronger binding and reduced molecular mobility of water molecules, reflecting a more stable system. Therefore, these minimum entropy values were considered optimal for maintaining product stability, ensuring safe storage, and prolonging shelf life (Pérez-Alonso et al., 2006; Escalona-García et al., 2016).

2.8. Calculation of adsorption surface area (ASA)

The adsorption surface area of RJ was computed using Eq. (8), and it involved the utilization of monolayer moisture content acquired from the GAB coefficients. This parameter gives crucial information to evaluate the water-binding capacity for RJ. The adsorption surface area is calculated by using the monolayer moisture content value, at each temperature, through Eq. (8) (Arslan-Tontul, 2020).

$$ASA = \frac{X_0 \times N_A \times A_m}{M(H_2O)} = 3.54 \times 10^3 \times X_0 \quad (8)$$

X_0: monolayer moisture content given by GAB model (kg (kg d. b.)$^{-1}$); N_A: Avogadro number 6.022 × 10^{23}mol^{-1}; A_m: Surface area of a water molecule (1.06 × 10^{-19} m^2); M (H_2O): Molar weight of water.

The calculation is based on the concept that X_0 represents the amount of water needed to cover all primary adsorption sites with a single molecular layer (Brunauer et al., 1938). When X_0 is converted to the actual number of water molecules (using Avogadro's number and the molar mass of water), and each molecule is known to occupy approximately 1.06 × 10^{-19} m^2 of surface (Timmermann et al., 2001), the product gives the total accessible surface area. This method has been successfully applied to various food materials for determining water-binding capacity (Aviara and Ajibola, 2002).

3. Results and discussion

3.1. Sorption isotherms

Fig. 1 shows the moisture sorption isotherms of royal jelly (RJ) at 30, 40, and 50 °C, indicating a positive relationship between equilibrium moisture content (X_{eq}) and water activity (a_w). As the water activity increased, the RJ absorbed more moisture, confirming that the rise in vapor pressure within the RJ is influenced by the higher vapor pressure of the surrounding environment. This observation aligns with findings from previous studies (Hssaini et al., 2022; Ouaabou et al., 2021a; Tagnamas et al., 2024). Sorption experiments were conducted over two to 3 weeks at each temperature to ensure equilibrium.

As shown in Fig. 1, the sorption isotherms exhibited a typical sigmoidal (Type II) shape according to the Brunauer classification, characteristic of food and bioproducts rich in sugars and proteins, corresponding to unrestricted monolayer-multilayer adsorption on an open and non-porous surface of the microcapsules. At low water activity (a_w < 0.3), water molecules are strongly bound to polar sites on the RJ matrix, forming a monolayer. As a_w increases (0.3 < a_w < 0.6), multilayer adsorption occurs, followed by a sharp rise in equilibrium moisture content at higher a_w values (a_w >0.6) due to capillary condensation and filling of microvoids.

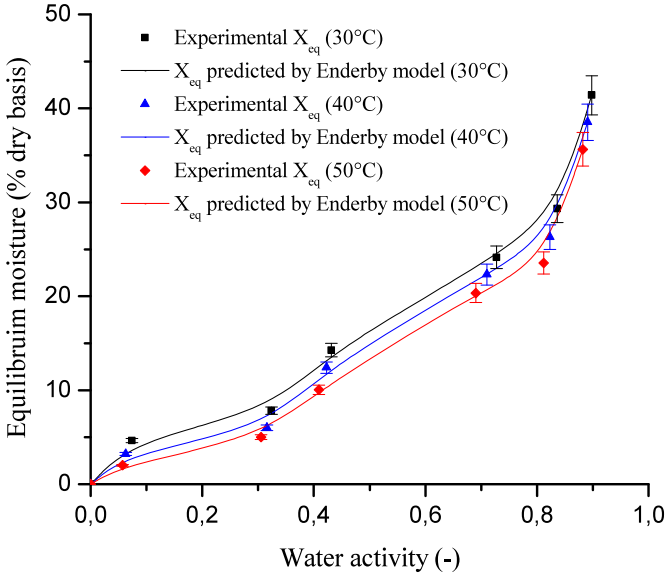

Fig. 1. Adsorption isotherms of royal jelly at 30, 40 and 50 °C.

This Type II behavior indicates that RJ binds water strongly at low humidity levels but becomes increasingly susceptible to moisture gain and degradation as a_w rises. Consequently, RJ exhibits higher physicochemical stability at low a_w, whereas above a_w = 0.6, increased molecular mobility and potential microbial activity may compromise product quality and shelf life. For this reason, maintaining a_w below approximately 0.3–0.4 is recommended to ensure optimal storage stability of freeze-dried RJ.

The sorption capacity of a material is closely linked to its biochemical composition and structural characteristics. In our study, we found that the hygroscopicity of RJ decreased with increasing temperatures, even at constant water activity levels. This can be explained by the fact that higher temperatures increase the energy and mobility of water molecules, causing them to move further apart. As a result, the water molecules become more prone to escaping their binding sites, reducing the amount of moisture retained. These results are consistent with previous research by Owo et al. (2017); Andres Collazos-Escobar et al. (2020); Moraes et al. (2024).

3.2. Modeling of the sorption isotherms

The moisture sorption behavior of royal jelly (RJ) was analyzed using five mathematical models to describe its sorption isotherms. The performance of each model was evaluated based on two key criteria: the minimum mean relative error (MRE) and the highest correlation coefficient (r), as outlined by (Ruiz-López and Herman-Lara, 2009). Among the tested models, the Enderby model provided the best fit to the experimental data, exhibiting the consistently high correlation coefficients (0.9853–0.9958) and competitive MRE values (1.7698–3.8968) across the studied temperatures (Table 3). Additionally, the Enderby model achieved superior average performance (mean

Table 3
Parameter estimates for royal jelly powder adsorption models at various temperatures.

	Model coefficients				Statistical parameters	
	a	b	C	d	R	MRE
	30°C					
GAB	X_0: 6.2691	k: 0.8860	C:12.6475		0.9767	3.9903
Halsey	4.6484	2.6381 × 10^8			0.9647	4.2453
Smith	2.7305	15.9096			0.958	4.6214
Enderby	79.1100	−5.4126	2.7250	1.0269	0.9853	3.8968
Caurie	1.1022	2.8390			0.9439	5.3237
	40°C					
GAB	X_0: 3.6404	k: 0.8852	C: 6.0305		0.9120	6.7188
Halsey	3.8983	47.1041			0.9640	3.7747
Smith	0.1049	14.0000			0.9269	5.3227
Enderby	−0.3949	1.1627	15.8380	0.5515	0.9958	1.8291
Caurie	0.1464	3.7240			0.9220	5.4926
	50°C					
GAB	X_0: 2.4619	k: 0.8850	C: 3.3066		0.9739	1.4791
Halsey	2.1426	2.5631 × 10^8			0.7315	3.7837
Smith	3.0876	5.8354			0.9545	1.6547
Enderby	−0.6487	−0.1263	18.6490	0.1278	0.9742	1.7698
Caurie	1.1027	1.8152			0.9674	1.4059

R = 0.9851, mean MRE = 2.50) compared to other models tested.

It should be noted that at 50 °C, the GAB and Caurie models exhibited slightly lower MRE values (1.4791 and 1.4059, respectively) compared to the Enderby model (1.7698). However, this apparent advantage must be interpreted in context. First, all models at 50 °C show substantially lower MRE values compared to lower temperatures due to the reduced magnitude of equilibrium moisture content at higher temperatures—since MRE is a relative error metric, lower moisture values inherently produce smaller relative errors for comparable absolute deviations. Second, when considering model consistency across the entire temperature range studied (30–50 °C), the Enderby model demonstrated more stable and physically meaningful parameter behavior, whereas GAB and Caurie parameters showed greater variability with temperature.

The superior performance of the Enderby model can be attributed to its ability to accurately capture both the initial steep adsorption at low water activity and the gradual multilayer adsorption at higher water activity, which is characteristic of RJ's sorption behavior. In contrast to simpler models, such as Halsey or Smith, the Enderby model accounts for the nonlinearity of the isotherm over the full water activity range, providing a more comprehensive description of water-binding mechanisms in complex matrices like RJ. These results were similar to those reported by Abdenouri et al. (2010), who found that the Enderby showed the best estimators for predicting the equilibrium moisture content of milk powder. A summary of the nonlinear regression analysis used to assess the alignment of the experimental data with the models is provided in Table 3.

Furthermore, the Enderby model parameters remained physically consistent and followed the same trend across temperatures, suggesting better predictive reliability and thermodynamic coherence than the alternative models. Therefore, despite the marginally higher MRE at 50 °C, the Enderby model was considered the most appropriate overall for describing RJ sorption behavior.

While the Enderby model was selected for its superior predictive performance, the GAB model remains valuable for extracting thermodynamic parameters, particularly the monolayer moisture content (X_0), which is used in subsequent calculations of adsorption surface area and integral thermodynamic properties.

The monolayer moisture content (X_0) is widely recognized as a critical indicator of food stability, as it represents the number of available sorption sites where water molecules can bind. Maintaining moisture levels below X_0 is essential to minimize degradation reactions. As shown in Table 3, the monolayer moisture content obtained from the GAB model decreased with rising temperatures. This reduction can likely be attributed to the weakening of specific bonds, such as hydrogen bonds, as temperature increases. Consequently, water molecules become less stable and are more prone to detachment from their binding sites within the food's matrix. The estimated X_0 values fell within the typical range reported for agro-food products, as noted by Lewicki, (1997a). Similar results were reported by Escalona-García et al. (2016) for chia oil microcapsules. Furthermore, the constant k of the GAB model exhibited an upward trend with increasing temperatures, consistent with observations in honey powder sorption studies (Mutlu et al., 2020). While, the parameter C, which is not influenced by temperature, remained within the expected range ($5.67 \leq C \leq \infty$), as described by Lewicki, (1997b). The parameter *k* reflects the multilayer adsorption enthalpy and quantifies the energy required for water molecule binding within this layer. In this study, no significant trend was observed between *k* values and temperature. Nevertheless, the GAB model proves particularly suitable for describing sigmoidal-type isotherms when *k* falls within the range of 0.24–1. For the RJ sample, the *k* values obtained at the three investigated temperatures satisfied this criterion (Lewicki, 1997a).

3.3. Integral thermodynamic properties of RJ

3.3.1. Spreading pressure

Fig. 2 shows the variation of spreading pressure with water activity (a_w) for royal jelly (RJ) at 30 °C, 40 °C and 50 °C. For all temperatures, spreading pressure increases monotonically with a_w, which is consistent with results reported for freeze dried oyster mushroom powder (Pascual-Pineda et al., 2021b), freeze dried cherry powder (Ouaabou et al., 2021a). However, spreading pressure decreases as temperature increases; the 30 °C series exhibits the highest values (≈0.10–0.16J.m^{-2}), followed by 40 °C (≈0.08–0.1J.m^{-2}) and 50 °C (≈0.06–0.11J.m^{-2}). This behavior indicates that, while higher water activity promotes surface accumulation of water, increasing temperature reduces the net adsorption at the surface likely because thermal agitation weakens water-RJ binding and promotes desorption from surface sites. This temperature-dependent behavior has been observed in other biopolymers such as carboxymethyl cellulose, guar, locust bean, and xanthan gums, as noted by Torres et al. (2012), Similar trends, where higher temperatures result in lower spreading pressure, were also reported for black pepper oleoresin encapsulated by spray drying (Pascual Pineda et al., 2021a)and spray dried coffee powder (Pascual-Pineda and Guerrero-Hernández, 2022).

These findings have important implications for RJ storage and handling. The lower spreading pressure at elevated temperatures indicates reduced water binding capacity, which could accelerate moisture-related quality deterioration. Therefore, maintaining storage temperatures at or below 30 °C would enhance RJ powder's resistance to environmental moisture uptake and improve long-term storage stability.

3.3.2. Integral enthalpy

The variation of integral enthalpy with equilibrium moisture content for royal jelly (RJ) at 30, 40, and 50 °C is shown in Fig. 3. The integral enthalpy is strongly negative (≈−35 to −40 kJ mol^{-1}) at very low moisture contents (X_{eq}<5 % d.b). As moisture content increases progressively, the enthalpy rises monotonically, becoming less negative and approaching values close to zero at higher equilibrium moisture contents (X_{eq}>15 %). This characteristic evolution of integral enthalpy reflects the thermodynamic nature of water-matrix interactions in RJ. At very low moisture contents, water molecules adsorb onto the most energetically favorable sites-primarily polar groups on proteins (amino and carboxyl groups) and hydroxyl groups on sugars (glucose, fructose). The highly negative enthalpy values in this region indicate that water adsorption is strongly exothermic, releasing substantial energy as water molecules form hydrogen bonds with these active sorption sites. This

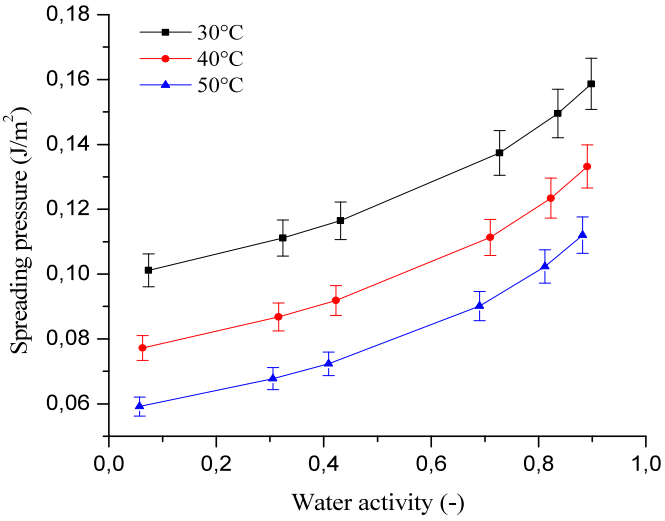

Fig. 2. Spreading pressure variation of royal jelly.

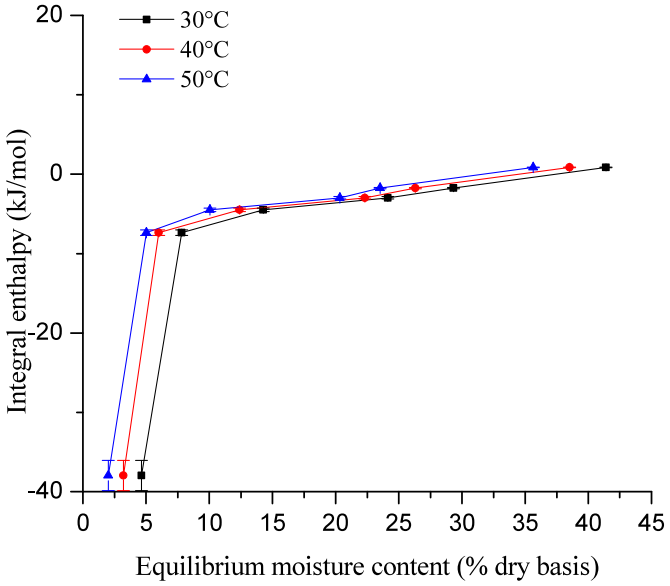

Fig. 3. Variation of integral enthalpy as a function of moisture content for royal jelly.

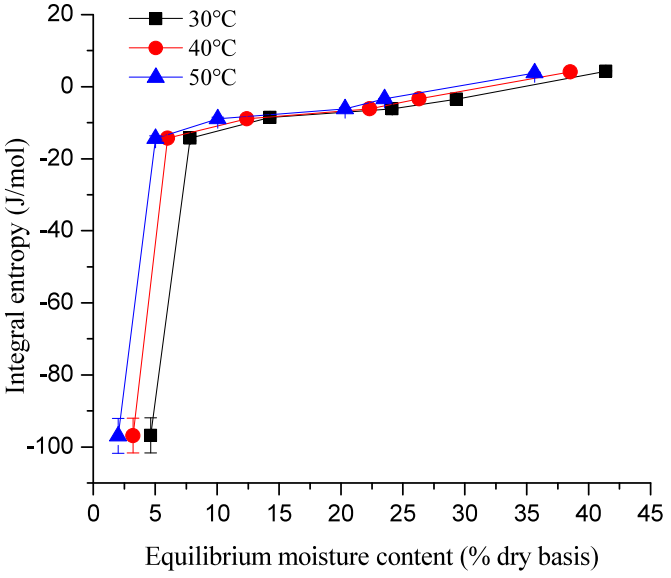

Fig. 4. Variation of integral entropy as a function of moisture content for royal jelly.

corresponds to monolayer adsorption, where water-matrix interactions dominate. As moisture content increases, the primary binding sites become saturated, and additional water molecules occupy progressively less energetic secondary sites or form multilayers through water-water hydrogen bonding. Consequently, the integral enthalpy becomes less negative, reflecting weaker binding forces and the transition from bound water to more loosely associated or free water. Such behavior is typical for sugar- and protein-rich matrices (Lewicki, 1997b; Mutlu et al., 2020)

From a drying perspective, the integral enthalpy profile has important practical implications. The strongly negative values at low moisture contents indicate that the final stages of drying, when removing tightly bound water from primary sorption sites require substantially higher energy input compared to the initial stages. During early drying, when moisture content is high, water exists primarily as free or weakly bound multilayer water with enthalpies near zero, which can be removed with relatively low energy. However, as drying progresses and moisture content decreases, the energy demand increases significantly due to the necessity of breaking strong water-matrix hydrogen bonds.

These insights suggest that RJ drying protocols should be designed in multiple stages: initial high-rate drying for free water removal, followed by carefully controlled final drying at moderate temperatures or extended times to prevent thermal degradation of heat-sensitive bioactive compounds (proteins, vitamins, enzymes) while ensuring adequate moisture removal for stability. Similarly, for storage optimization, the integral enthalpy data indicates that maintaining RJ at low moisture contents minimizes the risk of moisture gain from the environment, as the high energy barrier for water adsorption at these levels provides a natural protection against rehydration. Understanding these enthalpy-moisture relationships enables the design of energy-efficient processing and storage strategies that preserve RJ's bioactive integrity and functional quality throughout its shelf life.

3.3.3. *Integral entropy*

Fig. 4 presents the variation in integral enthalpy with the moisture content for royal jelly at 30 °C, 40 °C, and 50 °C. At lower moisture levels (X_{eq}<5 % d.b), the integral entropy shows highly negative values (≈-100J/mol), indicating strong water-matrix interactions where water molecules are tightly bound to primary adsorption sites. This strong binding severely restricts the rotational freedom and mobility of water molecules, resulting in low entropy and high molecular order.

As moisture content increases (X_{eq}>5 % d.b), the integral entropy rises sharply and then continues to increase more gradually. This transition reflects a fundamental change in the nature of water binding. The initial water molecules occupy the most energetically favorable sites on the solid surface, forming a bound monolayer. Once these primary sites are saturated, additional water molecules form secondary layers with progressively weaker binding energies, allowing greater molecular mobility and thus higher entropy. At higher moisture contents (above 30–35 % dry basis), the entropy approaches positive values, indicating that water behaves similarly to free liquid water with minimal restrictions on molecular movement.

The minimum point in the integral entropy curve, occurring at approximately 4–5 % moisture content (dry basis) with a value near −95 J/mol, represents the condition of maximum thermodynamic stability for RJ. At this critical moisture content, water molecules are optimally bound to the solid matrix, exhibiting minimal molecular mobility and reactivity. This state corresponds to the lowest chemical and microbiological activity, as the bound water is unavailable for participating in deteriorative reactions such as lipid oxidation, enzymatic degradation, or microbial growth. Therefore, this critical moisture range represents the optimal storage condition for maximizing shelf life and maintaining product quality (Ouaabou et al., 2021a; Iglesias et al., 2022; Tagnamas et al., 2024).

The three temperature curves (30 °C, 40 °C, and 50 °C) are remarkably similar and nearly superimposed throughout most of the moisture range, suggesting that temperature has a relatively minor effect on the entropy-moisture relationship within this experimental range. However, slight divergence is observed at higher moisture contents (above 35 %), where temperature may begin to influence the organization and mobility of weakly bound water.

From a practical standpoint, understanding the integral entropy behavior is crucial for establishing optimal storage and processing conditions for RJ. Storage conditions, particularly moisture content and water activity, play a critical role in maintaining product quality throughout the supply chain. These factors directly influence the water sorption behavior of the product during storage and transportation under varying temperature and humidity conditions. Beyond physicochemical stability, moisture content significantly impacts sensory attributes such as taste, aroma, texture, and color. Excessive moisture levels can promote microbial proliferation, enzymatic activity, and non-enzymatic browning reactions, all of which compromise product quality and safety (Iglesias et al., 2022).

The integral entropy analysis provides a thermodynamic framework for identifying the moisture content range that ensures maximum stability. Based on Fig. 4, maintaining RJ at moisture contents near the entropy minimum (4–5 % dry basis) would optimize storage stability by minimizing water availability for deteriorative reactions. However, rather than targeting a single precise value, it may be more practical to identify a stability range where entropy remains relatively low and stable, as the minimum is not sharply defined and slight variations in moisture content may be inevitable during storage. This approach offers a more robust strategy for quality preservation while accommodating the practical challenges of maintaining exact moisture levels in real-world storage conditions.

3.3.4. Adsorption surface area

The adsorption surface area of RJ was determined using the monolayer moisture content calculated from the GAB model. At temperatures of 30 °C, 40 °C, and 50 °C, the surface areas were measured as 221.93 m^2/g, 128.87 m^2/g, and 87.15 m^2/g, respectively. These findings indicate a clear decline in the hydrogen bonding capacity of RJ as the temperature increases. This reduction can be attributed to a decrease in the number of active binding sites, which is likely caused by physical and chemical changes in the material structure at elevated temperatures (Velázquez-Gutiérrez et al., 2015).

Several factors influence the water sorption behavior of RJ, including its chemical composition, structural morphology, and the nature of interactions between water molecules and the surface. As temperature rises, these interactions weaken, leading to a diminished ability of the material to adsorb water (Cadden, 1988). This decrease in water adsorption at higher temperatures directly affects RJ's stability, as moisture content outside the optimal range can accelerate chemical degradation, microbial growth, or texture changes. Understanding the relationship between temperature, water sorption, and equilibrium moisture content is therefore essential for predicting and enhancing the shelf-life and quality of RJ during storage and processing (Ouaabou et al., 2021a). The calculated values are consistent with those reported for other powdered food products, such as honey powder (Mutlu et al., 2020), onion powder (Majid et al., 2019), and cherry powder (Ouaabou et al., 2021a).

3.4. SEM analysis

Scanning electron microscopy (SEM) was used to investigate the microstructural changes in RJ after the adsorption process. The surface morphology of RJ is shown in Fig. 5, where the particles exhibit a clogging pattern as a result of water adsorption, making it difficult to distinguish individual particles. This phenomenon is explained by the high integral enthalpy of adsorption, which reflects the strong interaction between RJ particles and water molecules.

Li et al. (2025) described similar microstructural behaviour, employing SEM to reveal surface deformation and aggregation in hygroscopic materials exposed to moisture. Strong water-matrix interactions were ascribed to these morphological alterations, which were in line with high isosteric heat of sorption values. This confirms our finding that the high net isosteric heat of adsorption, which is a reflection of strong water binding forces, is associated with the clogging pattern in RJ particles (Fig. 5).

The SEM images reveal that the RJ particles are closely packed and agglomerated, with individual particles merging due to water adsorption. This results in a smoother, more uniform surface morphology. The formation of a thin layer of water over the RJ particles leads to agglomeration, altering the material's microstructure. These changes can significantly impact the flow properties, compaction behavior, and overall handling of RJ. In other hygroscopic materials, comparable morphological alterations brought on by moisture adsorption have been documented. Water has a major impact on the microstructure and surface morphology of maltodextrins, as demonstrated by Saavedra-Leos et al. (2024), who found that water adsorption caused structural rearrangements involving partial crystallization and particle agglomeration. In a different investigation, Saavedra-Leos et al. (2019) employed SEM to show surface smoothing and particle coalescence in spray-dried blueberry juice–maltodextrin systems subjected to moisture. They attributed these alterations to the development of a thin water film that encourages particle adhesion. These results are consistent with our SEM data, which showed that RJ's adsorption of water caused particle fusion and the formation of a smoother surface, which in turn affected the material's flowability and handling characteristics.

Understanding the adsorption behavior of RJ is essential for optimizing its use in applications that require moisture control, such as packaging, food technology, pharmaceuticals, and cosmetics. To mitigate excessive agglomeration, strategies like incorporating anti-caking agents or modifying environmental conditions could be considered. The SEM analysis highlights the importance of understanding these structural changes for improving the performance of RJ in moisture-sensitive applications. Comparable procedures for hygroscopic powders have been documented. Chang et al. (2018) looked at how anti-caking substances like calcium silicate and tricalcium phosphate affected the stability and microstructure of spray-dried soursop powder. According to their SEM research, these additions enhanced storage stability in humid environments and decreased particle agglomeration. These results provide support to the assumption that improving ambient humidity or adding anti-caking chemicals could improve RJ handling and performance in moisture-sensitive applications.

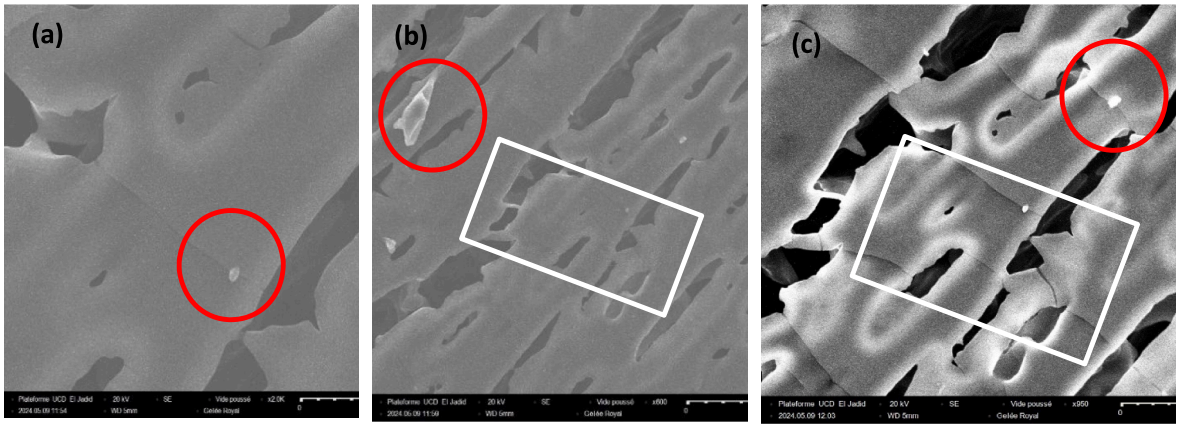

Fig. 5. Scanning electron microscopy images of freeze-dried of the royal jelly lyophilized powder at different magnifications: (a) × 2.0K, (b) × 600K, and (c) × 950K. The white square in (c) highlights a region exhibiting an interconnected fibrillary network (red circles) with associated knob-like structures (arrowheads).

3.5. Thermal behavior

The sample's thermal characteristics were examined through thermogravimetric analysis (TGA) and differential thermal analysis (DTA), with the resulting thermal curve presented in Fig. 6. The TGA curve exhibits three separate phases of weight loss, identified from the inflection points of the derivative thermogravimetry (DTG) curve. The first region, occurring between 36 °C and 137 °C, shows a 6 % mass loss, primarily due to the elimination of physically adsorbed water and other volatile substances. This finding directly corroborates the sorption isotherm data, confirming that the initial mass loss is associated with the removal of loosely bound water, consistent with the water molecules described in the multilayer and capillary condensation regions of the Type II isotherm. The second region, from 137 °C to 246 °C, exhibits a more significant mass loss of 28 %, likely due to the volatilization of polysaccharides such as pectin, which undergo decarboxylation. Various biopolymeric and plant-derived materials have been shown to exhibit comparable thermal breakdown behaviour. In their TGA/DTG analysis of citrus pomace rich in pectin and lignocellulose, Zannini et al. (2021) found weight loss phases linked to water evaporation and polysaccharide breakdown, which is in line with the first two degradation zones seen in this investigation. Similar multi-step degradation patterns in olive pomace and activated carbon generated from it were also found by Alouiz et al. (2024), who attributed the first stage of mass loss to moisture removal and the second stage to the thermal breakdown of hemicellulosic and cellulosic components. These results support our findings, which show that the evaporation of physically bound water and the subsequent breakdown of polysaccharides like pectin and related organic ingredients are responsible for the early weight loss of RJ.

The third and final region, between 246 °C and 800 °C, accounts for the largest mass loss 84 %. This substantial reduction is associated with the thermal degradation of the remaining organic material, leaving behind a stable residue. By 800 °C, nearly all of the initial mass has been lost, indicating complete thermal decomposition. Similar trends have been observed in tropical fruit powders, further validating these findings, comparable high-temperature degradation patterns have been reported for other organic and polysaccharide-rich materials. Ramos et al. (2020) observed up to 90 % mass loss in Amazonian starches by 700 °C, corresponding to the decomposition of starch macromolecules. Gola et al. (2024) similarly described an 81–90 % mass loss between 318 °C and 750 °C in thermally sensitive polymers, indicating nearly complete polymer decomposition. In addition, Feitoza et al. (2022) reported a major weight loss (≈89 %) between 803 °C and 957 °C during the thermal degradation of biochar, confirming full carbon decomposition at 1000 °C. These findings align with the present TGA results, where the third degradation stage of RJ corresponds to the complete breakdown of its organic constituents, leaving only a stable residual fraction.

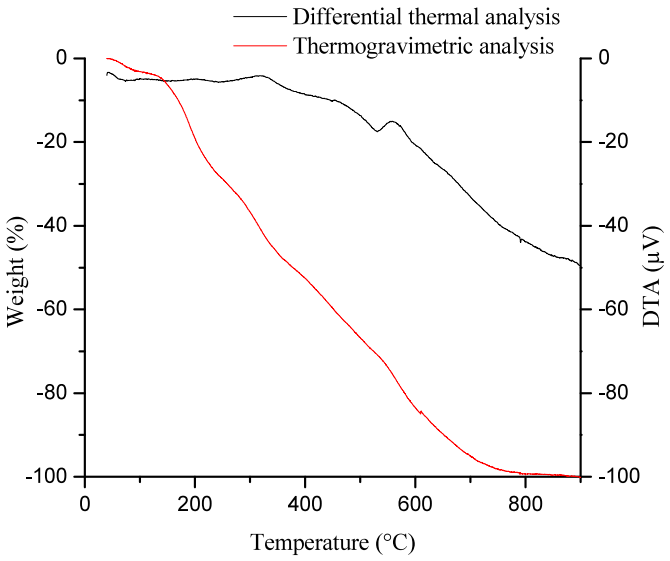

Fig. 6. Thermogravimetry analysis of royal jelly powder.

The DTA complements the TGA by detecting temperature differences between the sample and an inert reference as they are heated. The DTA curve shows peaks corresponding to thermal events like melting, crystallization, or chemical reactions. A peak in the DTA curve, confirming whether the loss is exothermic or endothermic, mirrors each weight loss detected by TGA. When examining thermal degradation processes, the relationship between TGA and DTA data is especially noticeable. According to Isik et al. (2025), TGA curves usually show discrete weight loss regions that correspond to various thermal and chemical processes, and DTA peaks closely match these weight loss regions. As an illustration, the TGA curve for nylon 6 analysis reveals a considerable mass loss between 350 °C and 500 °C, which is directly correlated with endothermic peaks in the DTA curve that are ascribed to high-temperature decomposition (Yang et al., 2025)

Both, the TGA and DTA analyses provide a comprehensive understanding of the sample's thermal stability and decomposition behavior. The three distinct regions of weight loss correspond to different stages of thermal decomposition: the evaporation of volatiles, decomposition of organic compounds, and the final breakdown. The strong correlation between TGA's mass loss data and DTA's thermal events enhances the reliability of these results, with TGA offering quantitative insight into mass loss and DTA qualitatively confirming the associated thermal processes.

4. Conclusion and perspectives

This study demonstrates that the equilibrium moisture content (X_{eq}) of royal jelly (RJ) increases with rising water activity (a_w), while at a constant water activity, the hygroscopicity of RJ decreases with temperature. The sorption isotherms were identified as Type II according to Brunauer's classification, typical of food materials with a significant mesoporous structure. The monolayer moisture content (X_0), determined using the GAB model, ranged from 6.27 % at 30 °C to 2.46 % (dry basis) at 50 °C, reflecting temperature-dependent reduction in available sorption sites.

Among the five models tested (GAB, Halsey, Smith, Enderby, and Caurie), the Enderby equation provided superior predictive accuracy across all temperatures, with correlation coefficients ranging from 0.9742 to 0.9958 and mean relative errors between 1.77 and 3.90. The model's consistent performance across the entire water activity range (0.05–0.90) makes it the recommended choice for predicting RJ moisture sorption behavior.

The thermodynamic analysis revealed critical insights for RJ preservation. The integral enthalpy ranged from −35 to −40 kJ mol^{-1} at low moisture contents (<5 % d.b.), indicating strong water-matrix interactions at primary sorption sites. These highly negative values demonstrate that the final drying stages require substantially higher energy input due to the need to break strong hydrogen bonds. The integral entropy analysis identified a minimum value of approximately −95 J/mol at 4–5 % moisture content (dry basis), corresponding to relative humidity between 0.15 and 0.23. This minimum entropy point represents the optimal storage condition where water molecules exhibit minimal mobility and reactivity, ensuring maximum physicochemical stability and extended shelf life.

SEM analysis revealed an agglomerated particle structure resulting from water adsorption-induced particle fusion, with formation of a thin water film promoting coalescence. These microstructural changes directly impact powder flowability and handling characteristics. TGA-DTA analysis demonstrated three distinct thermal degradation stages: initial mass loss of 6 % (36–137 °C) attributed to physically adsorbed water removal, consistent with multilayer water described in sorption

isotherms; secondary mass loss of 28 % (137–246 °C) corresponding to polysaccharide decomposition; and final mass loss of 84 % (246–800 °C) representing complete organic material breakdown.

Beyond these fundamental insights, the present work highlights the engineering and technological relevance of these findings. The detailed characterization of RJ's sorption and thermodynamic properties establishes critical design parameters for optimizing drying, packaging, and storage conditions. The identified enthalpy–moisture relationships provide a scientific basis for implementing energy-efficient drying protocols and humidity-controlled storage systems that prevent degradation of heat-sensitive bioactives. By coupling empirical sorption data with thermodynamic modeling, this study bridges fundamental food-physics understanding and industrial process design, offering a predictive framework for moisture management and stability control in royal-jelly powders. Consequently, these findings contribute to advancing innovative preservation strategies for high-value natural products in the pharmaceutical, nutraceutical, and agro-industrial sectors.

CRediT authorship contribution statement

Rachida Ouaabou: Methodology, Investigation, Data curation, Formal analysis, Software, Writing – original draft. **Lahcen Hssaini:** Formal analysis. **Abderrahim Alahyane:** Conceptualization. **Abdessamad Lahrach:** Conceptualization. **Nadia Massaoudi:** Formal analysis. **Jalal Isaad:** Supervision. **EL amine Ajal:** Data curation. **Aadil Bajoub:** Software. **Said Ennahli:** Conceptualization, Methodology, Funding acquisition, Writing – review & editing.

Funding

This work was supported by the PRIMA-2022 program (TECHONEY) and funded in Morocco by the Ministry of Higher Education, Scientific Research and Innovation (MESRSI) **(Agreement 1733).**

Declaration of competing interest

The authors declare that they have no known competing financial interests or personal relationships that could have appeared to influence the work reported in this paper.

Data availability

No data was used for the research described in the article.

References

Abdenouri, N., Idlimam, A., Kouhila, M., 2010. Sorption isotherms and thermodynamic properties of powdered milk. Chem. Eng. Commun. 197, 1109–1125. https://doi.org/10.1080/00986440903412936. SUBPAGE:STRING:ACCESS.

Alouiz, I., Benhadj, M., Dahmane, E., Sennoune, M., Amarouch, M.Y., Mazouzi, D., 2024. Elaboration of fibrous structured activated carbon from olive pomace via chemical activation and low-temperature pyrolysis. Heliyon 10, e38886. https://doi.org/10.1016/j.heliyon.2024.e38886.

Andres Collazos-Escobar, G., Gutierrez Guzman, N., Alexander Vaquiro Herrera, H., Milena Amorocho Cruz, C., 2020. Moisture dynamic sorption isotherms and thermodynamic properties of parchment specialty coffee (Coffea arabica L.). Coffee Sci 15, 1–10. https://doi.org/10.25186/.v15i.1684.

Arslan-Tontul, S., 2020. Moisture sorption isotherm, isosteric heat and adsorption surface area of whole chia seeds. Lebensm. Wiss. Technol. 119, 108859. https://doi.org/10.1016/j.lwt.2019.108859.

Aviara, N.A., Ajibola, O.O., 2002. Thermodynamics of moisture sorption in melon seed and cassava. J. Food Eng. 55, 107–113. https://doi.org/10.1016/S0260-8774(02)00023-7.

Aviara, N.A., Igbeka, J.C., 2016. Modeling for drying of thin layer of native cassava starch in tray dryer. J. Biosyst. Eng. 41, 342–356. https://doi.org/10.5307/JBE.2016.41.4.342.

Brunauer, S., Emmett, P.H., Teller, E., 1938. Adsorption of gases in multimolecular layers. ACS Publ. 60, 309–319. https://doi.org/10.1021/JA01269A023.

Cadden, A.-M., 1988. Moisture sorption characteristics of several food fibers. J. Food Sci. 53, 1150–1155. https://doi.org/10.1111/J.1365-2621.1988.TB13550.X;WGROUP:STRING:PUBLICATION.

Castillo, M.D., Martínez, E.J., González, H.H.L., Pacin, A.M., Resnik, S.L., 2003. Study of mathematical models applied to sorption isotherms of Argentinean black bean varieties. J. Food Eng. 60, 343–348. https://doi.org/10.1016/S0260-8774(03)00008-6.

Chang, L.S., Karim, R., Abdulkarim, S.M., Yusof, Y.A., Ghazali, H.M., 2018. Storage stability, color kinetics and morphology of spray-dried soursop (Annona muricata L.) powder: effect of anticaking agents. Int. J. Food Prop. 21, 1937–1954. https://doi.org/10.1080/10942912.2018.1510836;JOURNAL:JOURNAL:LJFP20;REQUESTEDJOURNAL:JOURNAL:LJFP20;WGROUP:STRING:PUBLICATION.

Chen, L., Ning, F., Zhao, L., Ming, H., Zhang, J., Yu, W., Yi, S., Luo, L., 2023. Quality assessment of royal jelly based on physicochemical properties and flavor profiles using HS-SPME-GC/MS combined with electronic nose and electronic tongue analyses. Food Chem. 403, 134392. https://doi.org/10.1016/j.foodchem.2022.134392.

Escalona-García, L.A., Pedroza-Islas, R., Natividad, R., Rodríguez-Huezo, M.E., Carrillo-Navas, H., Pérez-Alonso, C., 2016. Oxidation kinetics and thermodynamic analysis of chia oil microencapsulated in a whey protein concentrate-polysaccharide matrix. J. Food Eng. 175, 93–103. https://doi.org/10.1016/J.JFOODENG.2015.12.009.

Feitoza, U., dos, S., Thue, P.S., Lima, E.C., dos Reis, G.S., Rabiee, N., de Alencar, W.S., Mello, B.L., Dehmani, Y., Rinklebe, J., Dias, S.L.P., 2022. Use of biochar prepared from the Açaí seed as adsorbent for the uptake of catechol from synthetic effluents. Molecules 27, 7570. https://doi.org/10.3390/molecules27217570.

Francisco-Ponce, B.A., Jiménez-Hernández, J., Arámbula-Villa, G., Flores-Andrade, E., Salazar, R., 2025. Influence of water activity on powder flow properties of nixtamalized corn and wheat flours. J. Cereal. Sci. 126, 104293. https://doi.org/10.1016/J.JCS.2025.104293.

Fratini, F., Cilia, G., Mancini, S., Felicioli, A., 2016. Royal Jelly: an ancient remedy with remarkable antibacterial properties. Microbiol. Res. 192, 130–141. https://doi.org/10.1016/j.micres.2016.06.007.

Gola, A., Pietrańczyk, R., Musiał, W., 2024. Synthesis and physicochemical properties of thermally sensitive polymeric derivatives of N-vinylcaprolactam. Polymers 16, 1917. https://doi.org/10.3390/POLYM16131917.

Halsey, G., 1948. Physical adsorption on non-uniform surfaces. J. Chem. Phys. 16, 931–937. https://doi.org/10.1063/1.1746689.

Hssaini, L., Ouaabou, R., Charafi, J., Idlimam, A., Lamharrar, A., Razouk, R., Hanine, H., 2022. Hygroscopic proprieties of fig (Ficus carica L.): mathematical modelling of moisture sorption isotherms and isosteric heat kinetics. South Afr. J. Bot. 145, 265–274. https://doi.org/10.1016/j.sajb.2020.11.026.

Iglesias, H.A., Baeza, R., Chirife, J., 2022. A Survey of temperature effects on GAB monolayer in foods and minimum integral entropies of sorption: a review. Food Bioproc. Techn ol. 15 (4 15), 717–733. https://doi.org/10.1007/S11947-021-02740-W.

Isik, M., Altuntas, G., Gasanly, N.M., 2025. Exploring the thermal properties of gallium sulfide (GaS) for high-temperature applications. Appl. Phys. A 131 (6), 1–7. https://doi.org/10.1007/S00339-025-08555-2.

Jung, H., Lee, Y., Yoon, W., 2018. Effect of moisture content on the grinding process and powder properties in food: a review. Processes 6, 69. https://doi.org/10.3390/pr6060069.

Khazaei, M., Ansarian, A., Ghanbari, E., 2018. New findings on biological actions and clinical applications of royal jelly: a review. J. Diet. Suppl. 15, 757–775. https://doi.org/10.1080/19390211.2017.1363843.

Lewicki, P.P., 1997a. The applicability of the GAB model to food water sorption isotherms. Int. J. Food Sci. Technol. 32, 553–557. https://doi.org/10.1111/j.1365-2621.1997.tb02131.x.

Lewicki, P.P., 1997b. Water sorption isotherms and their estimation in food model mechanical mixtures. J. Food Eng. 32, 47–68. https://doi.org/10.1016/S0260-8774(97)00002-2.

Li, S., Ge, H., Wang, H., 2025. Hygroscopic properties modeling and thermodynamic analysis of a seamless popping capsule. Sci. Rep. 15 (1), 1–16. https://doi.org/10.1038/s41598-025-15452-4.

Majid, I., Hussain, S., Nanda, V., 2019. Moisture sorption isotherms and quality characteristics of onion powder during storage as affected by sprouting. J. Food Meas. Char. 13, 775–784. https://doi.org/10.1007/s11694-018-9990-2.

Melliou, E., 2014. Chemistry, I.C.-S. in N.P. In: Undefined, 2014. Chemistry and Bioactivities of Royal Jelly. Elsevier, pp. 261–290. https://doi.org/10.1016/B978-0-444-63430-6.00008-4.

Moraes, M.S. de, Queiroz, A.J. de M., Figueirêdo, R.M.F. de, Matos, J.D.P. de, Silva, L.P.F.R. da, Santos, F.S. dos, Silva, S. do N., Oliveira, A.P. de, 2024. Water adsorption isotherms and thermodynamic properties of germinated pumpkin seeds flours. Revista Ciência Agronômica 55, e2028373. https://doi.org/10.5935/1806-6690.20240011.

Moraga, G., Igual, M., García-Martínez, E., Mosquera, L.H., Martínez-Navarrete, N., 2012. Effect of relative humidity and storage time on the bioactive compounds and functional properties of grapefruit powder. J. Food Eng. 112, 191–199. https://doi.org/10.1016/j.jfoodeng.2012.04.002.

Mutlu, C., Koç, A., Erbaş, M., 2020. Some physical properties and adsorption isotherms of vacuum-dried honey powder with different carrier materials. Lebensm. Wiss. Technol. 134, 110166. https://doi.org/10.1016/j.lwt.2020.110166.

Ornelas-Paz, J. de J., Yahia, E.M., 2014. Effect of the moisture content of forced hot air on the postharvest quality and bioactive compounds of mango fruit (Mangifera indica L. cv. Manila). J. Sci. Food Agric. 94, 1078–1083. https://doi.org/10.1002/jsfa.6384.

Ouaabou, R., Ennahli, S., Di Lorenzo, C., Hanine, H., Bajoub, A., Lahlali, R., Idlimam, A., Ait Oubahou, A., Mesnaoui, M., 2021. Hygroscopic properties of sweet cherry powder: thermodynamic properties and microstructural changes. J. Food Qual. 2021, 1–11. https://doi.org/10.1155/2021/3925572.

Ouaabou, R., Ennahli, S., Hssaini, L., Nabil, B., Idlimam, A., Lamharrar, A., Mahrouz, M., Hanine, H., 2022. Moisture sorption isotherms of sweet cherry (Prunus Avium L.): comparative study of kinetics and thermodynamic modeling of five varieties. Int. J. Food. Sci. 1–14. https://doi.org/10.1155/2022/6786590.

Owo, H.O., Adebowale, A.A., Sobukola, O.P., Obadina, A.O., Kajihausa, O.E., Adegunwa, M.O., Sanni, L.O., Tomlins, K., 2017. Adsorption isotherms and thermodynamics properties of water yam flour. Qual. Assur. Saf. Crop Foods 9, 221–227. https://doi.org/10.3920/QAS2015.0655.

Pascual Pineda, L.A., Contreras, Y.M., de Lourdes Arévalo Galarza, M., Morales, M.C., Marañón, A.H., Rascón Díaz, M.P., Andrade, E.F., 2021a. Clustering function and minimum change in spreading pressure as key factor to predict storage conditions for black pepper oleoresin encapsulated by spray drying. Food Biosci. 42, 101215. https://doi.org/10.1016/J.FBIO.2021.101215.

Pascual-Pineda, L., Guerrero-Hernández, A., 2022. Determination of the spreading pressure and shelf-life of spray-dried coffee powder: quality assurance of a water-soluble food Determinación de la presión de. rmiq.org 21, 2921. https://doi.org/10.24275/rmiq/Alim2921.

Pascual-Pineda, L.A., Hernández-Marañon, A., Castillo-Morales, M., Uzárraga-Salazar, R., Rascón-Díaz, M.P., Flores-Andrade, E., 2021b. Effect of water activity on the stability of freeze-dried oyster mushroom (Pleurotus ostreatus) powder. Dry. Technol. 39, 989–1002. https://doi.org/10.1080/07373937.2020.1739064;WGROUP:STRING:PUBLICATION.

Pérez-Alonso, C., Beristain, C.I., Lobato-Calleros, C., Rodríguez-Huezo, M.E., Vernon-Carter, E.J., 2006. Thermodynamic analysis of the sorption isotherms of pure and blended carbohydrate polymers. J. Food Eng. 77, 753–760. https://doi.org/10.1016/j.jfoodeng.2005.08.002.

Popovski, D., Mitrevski, V., 2004. Some new four parameter models for moisture sorption isotherms. Electron. J. Environ. Agric. Food Chem. 3 (3), 698–701.

Ramadan, M.F., Al-Ghamdi, A., 2012. Bioactive compounds and health-promoting properties of royal jelly: a review. J. Funct.Foods 4, 39–52. https://doi.org/10.1016/j.jff.2011.12.007.

Ramanathan, A.N.K.G., Nair, A.J., Sugunan, V.S., 2018. A review on Royal Jelly proteins and peptides. J. Funct.Foods 44, 255–264. https://doi.org/10.1016/j.jff.2018.03.008.

Ramos, A. da S., Verçosa, R. de M., Teixeira, S.M.L., Teixeira-Costa, B.E., 2020. Calcium oxalate content from two Amazonian amilaceous roots and the functional properties of their isolated starches. Food Sci. Technol. 40, 705–711. https://doi.org/10.1590/FST.18419.

Ratti, C., 2001. Hot air and freeze-drying of high-value foods: a review. J. Food Eng. 49, 311–319. https://doi.org/10.1016/S0260-8774(00)00228-4.

Ruiz-López, I.I., Herman-Lara, E., 2009. Statistical indices for the selection of food sorption isotherm models. Dry. Technol. 27, 726–738. https://doi.org/10.1080/07373930902827932.

Saavedra-Leos, M.Z., Leyva-Porras, C., López-Martínez, L.A., González-García, R., Martínez, J.O., Compeán Martínez, I., Toxqui-Terán, A., 2019. Evaluation of the spray drying conditions of blueberry Juice-Maltodextrin on the yield, content, and retention of Quercetin 3-d-Galactoside. Polymers 11, 312. https://doi.org/10.3390/polym11020312.

Saavedra-Leos, Z., Carrizales-Loera, A., Lardizábal-Gutiérrez, D., López-Martínez, L.A., Leyva-Porras, C., 2024. Exploring the equilibrium state diagram of maltodextrins across diverse dextrose equivalents. Polymers 16, 2014. https://doi.org/10.3390/POLYM16142014.

Smith, S.E., Smith, S.E., 1947. The sorption of water vapor by high polymers. J. Am. Chem. Soc. 69, 646–651. https://doi.org/10.1021/ja01195a053.

Tagnamas, Z., Idlimam, A., Lamharrar, A., 2024. Hygroscopic analysis of pre-dried madder roots (Rubia tinctorum L.) using a solar dryer: implications for safe storage conditions. J. Clean. Prod. 434, 139848. https://doi.org/10.1016/j.jclepro.2023.139848.

Timmermann, E.O., Chirife, J., Iglesias, H.A., 2001. Water sorption isotherms of foods and foodstuffs: BET or GAB parameters? J. Food Eng. 48, 19–31. https://doi.org/10.1016/S0260-8774(00)00139-4.

Torres, M.D., Moreira, R., Chenlo, F., Vázquez, M.J., 2012. Water adsorption isotherms of carboxymethyl cellulose, guar, locust bean, tragacanth and xanthan gums. Carbohydr. Polym. 89, 592–598. https://doi.org/10.1016/j.carbpol.2012.03.055.

Van Den Berg, C., Bruin, S., 1981. Water activity and its estimation in food systems: theoretical aspects. In: Water Activity: Influences on Food Quality. Elsevier, pp. 1–61. https://doi.org/10.1016/b978-0-12-591350-8.50007-3.

Velázquez-Gutiérrez, S.K., Figueira, A.C., Rodríguez-Huezo, M.E., Román-Guerrero, A., Carrillo-Navas, H., Pérez-Alonso, C., 2015. Sorption isotherms, thermodynamic properties and glass transition temperature of mucilage extracted from chia seeds (Salvia hispanica L.). Carbohydr. Polym. 121, 411–419. https://doi.org/10.1016/J.CARBPOL.2014.11.068.

Yang, Y., Li, Xinyu, Li, Z., Li, M., Chen, Y., Tan, S., Yu, H., Xu, P., Li, Xinxin, 2025. Integrated microcantilever for joint thermal analysis of trace hazardous materials. Sensors 2025 25. https://doi.org/10.3390/S25103004, 3004 25, 3004.

Zannini, D., Dal Poggetto, G., Malinconico, M., Santagata, G., Immirzi, B., 2021. Citrus pomace biomass as a source of pectin and lignocellulose fibers: from waste to upgraded biocomposites for mulching applications. Polymers 13, 1280. https://doi.org/10.3390/POLYM13081280, 13, 1280.